



### Science Arts & Métiers (SAM)

is an open access repository that collects the work of Arts et Métiers Institute of Technology researchers and makes it freely available over the web where possible.

This is an author-deposited version published in: <https://sam.ensam.eu>  
Handle ID: <http://hdl.handle.net/10985/24682>



This document is available under CC BY-NC-ND license

#### To cite this version :

Lucas RANCHIN, Fabien VIPREY, Guillaume FROMENTIN, Eric MONTEIRO, Philippe LORONG, Habib KARAOUNI, Théo DORLIN - Characterization of the clamping and internal residual stresses effects on the distortion of Inconel 718 parts resulting from turning - In: Machining Innovations Conference for Aerospace Industry, France, 2023-11-30 - MIC Procedia (2023) 085–092 - 2023

Any correspondence concerning this service should be sent to the repository

Administrator : [scienceouverte@ensam.eu](mailto:scienceouverte@ensam.eu)



# Characterization of the clamping and internal residual stresses effects on the distortion of Inconel 718 parts resulting from turning.

23<sup>rd</sup> Machining Innovations Conference for Aerospace Industry 2023 (MIC 2023),  
29<sup>th</sup> and 30<sup>th</sup> November 2023, Hannover, Germany

**Lucas Ranchin<sup>\*(a), (b)</sup>, Fabien Viprey<sup>(a)</sup>, Guillaume Fromentin<sup>(a)</sup>, Eric Monteiro<sup>(c)</sup>, Philippe Lorong<sup>(c)</sup>, Habib Karaoui<sup>(b)</sup>, Théo Dorlin<sup>(b)</sup>**

*(a) Arts et Métiers Institute of Technology, LABOMAP, Université Bourgogne Franche-Comté, HESAM Université, F-71250 Cluny, France*

*(b) Safran S.A, Research & Technology Center, F-78772, Magny-Les-Hameaux, France*

*(c) Laboratoire PIMM, Arts et Metiers Institute of Technology, CNRS, Cnam, HESAM Université, 151 boulevard de l'Hopital, F-75013 Paris, France*

\* Corresponding author: E-mail address: [lucas.ranchin@ensam.eu](mailto:lucas.ranchin@ensam.eu)

---

## Abstract

The understanding of phenomena related to machining processes in the aerospace industry is still the subject of study in the research community. This is due to the constrained geometric tolerances to ensure optimal performance and safety. Few studies have yet focused on the effect of the clamping sequence on part distortions during the machining process. Thus, the development of machining sequences, in particular the positioning of clamping points, still requires optimisation regarding the geometry to be machined. This contribution focuses on a first step of a study that aims to characterize workpiece distortions resulting from a multi-stage process in relation to the clamping, cutting forces and the initial or machining induced stresses. To validate the approach, a *in situ* methodology for characterising the defects has been developed alongside a particular workpiece holder based on an industrial procedure is set up in order to observe and limit the part distortion along the whole process. The machining sequence is divided into two machining steps separated by unclamping and clamping operations. Frontal axisymmetric grooves are machined in turning on both sides of a thin Inconel 718 elementary disks. These operations are subject to *in situ* measurement on both side of the workpiece. A laser profilometer and laser point sensors are used between each pass and at each stage of the machining sequence operation. The collected data will be used in a next step to validate a numerical model that predicts the evolution of the distortions of the part during the entire machining process.

© 2023 The Authors. Published by SSRN, available online at <https://www.ssrn.com/link/MIC-2023.html>

This is an open access article under the CC BY-NC-ND license (<http://creativecommons.org/licenses/by-nc-nd/4.0/>)

Peer review statement: Peer-review under responsibility of the scientific committee of the 23<sup>rd</sup> Machining Innovations Conference for Aerospace Industry 2023

**Keywords:** Inconel 718, turning, *in situ* measurement; distortions; machining sequence, clamping, Numerical simulation

---

## 1. Introduction

Today, many parts of revolutions are affected by multi-step machining (turbine disc, landing gear half-wheel,

etc.). However, the simulation of these machining stages has not yet been perfected. In fact, clamping is modelled in an elementary way and the multi-stage machining is often ignored. The clamping conditions are assumed to have no

impact on the deformation. In addition, the respect of tolerances is one of the most important issues when machining high values parts. There are many mechanisms involved in the machining process that can lead to geometric errors, in particular for thin parts. One of these phenomena is the rebalancing of initial residual stresses (*i.e.* bulk residual stress). The rebalancing leads to modification of the part geometry during the machining step and after unclamping. This phenomenon is the subject of numerous studies in the literature.

A state-of-the-art review of distortions caused by machining and initial residual stresses can be found in [1]. For example, [2] estimates that 90% of permanent distortions are related to residual stresses. However, the thickness of the part, internal residual stresses or machining stresses does not have the same asset. [3] found that internal residual stresses have an influence even on thin parts, which changes with the stress distribution. Some authors such as [4] demonstrated a limit (3-4 mm thickness) below which machined residual stresses become dominant.

However, [5] observed a material removal threshold after which the deformations become stable. This threshold is at 50-60% material removal (in terms of volume) and is said to be dependent on the internal stress state of the part.

Other studies focus on optimising the material removal strategy. For example, this is the case of [6] or [7] where different strategies for machining grooves in an aluminium (or steel) plate are tested. Thus, depending on the order in which the grooves are machined and on the remaining thickness at the end, the observed deformations are no longer the same.

Clamping is also a key factor in machining operation. For example, [8] estimated that up to 40% of part rejections are associated with clamp design. The work of [9] proposes a method, for thin turning parts, to evaluate the performance of the clamping designed and particularly the impact on the deformations after clamping. An optimal number of brackets to ensure good system balance and minimise geometric error can then be determined. However, most of the work focuses on the design of the clamps.

In recent years, new studies focused on clamping strategies using instrumented clamps. [10] and [7], developed a complex clamping system for an Inconel part. The configuration being hyperstatic, such that geometric defects will appear during clamping. Thus, the objective is to control the clamping force to minimise the defects before machining. Developments concerning in-process compensation are also appearing. This is the case of the work of [11] where a clamping system is composed of flexible fixtures with force sensors and motors. A touch probe is used to control the geometry of the part between the different passes. Two action levers are used to compensate defects. The clamps are reoriented and adjusted to compensate any defects that occur, and the machining strategy and tool path are modified accordingly.

Another alternative has been developed by [12]. They also propose an in-process method for testing the effect of residual stresses (bulks and machining). This process is compared to two tests. One involves releasing the machining

residual stresses and the initial residual stresses after rough machining. The aim is to re-establish the balance of forces between the two types of stress throughout the process. To achieve this, the first experiment is based on clamps whose applied forces are controllable, while the second consists of machining the part in one stage with adjustment of the clamps in accordance with the deformations measured at the control point. As a result, the reduction in distortion measured was 18.3% and 42.9% respectively compared with the tests carried out previously.

The nature of the machined material also plays an important role in the evolution of the stresses within a part. For example, for Inconel 718 the machining step introduces residual machining stresses that can lead to significant geometric defects. Cutting conditions and tool wear are significant factors that need to be monitored. As shown in [13], an important wear effect is related to geometrical defects. The studies [14-18] insist on the modification of the residual stress state. Compressive stresses are favoured in the subsurface while a more important tensile peak is observed at the surface. These changes in the stress state impacts the geometry of the part with machining and unclamping.

The objective of the current study is to characterize and quantify the geometric defects arising from stress state evolution inside machined parts when several machining operations and several clamping and unclamping steps are needed. This contribution deals with a first step of this study and focuses on a disk that is assumed to be free of internal residual stresses. This makes it possible to isolate the effect of the machining induced stresses and, in this context, the effect of machining strategy. Machining will be carried out in two machining steps, allowing the introduction of several "clamping, unclamping and reclamping steps". Precautions will be taken to limit the effect of deformation under cutting forces. The design chosen for the experimental device as well as the first observations concerning the deformation of the part are described in the following.

## 2. Experimental set-up

Thin disks of Inconel 718 (heat treated) to 45 HRC are used to perform tests. The geometry of the disk is described in Fig. 1. Two axisymmetric grooves are machined on the front face and back face, in two different stages. The lengths and depths of the grooves were determined by numerical simulation with the finite element software Morfeo© to evaluate distortions resulting from a heat treatment simulation and then rebalancing internal stresses. Both grooves do not overlap to minimize deformations under cutting forces. Indeed, the workpiece is set up to avoid elastic deformation under the cutting forces. The workpiece is pressed against the platen to limit deformation in the direction of the penetration force. Moreover, when the part is brought into position, there is no elastic deformation (apart from under its own weight, but this is negligible). Holding in position can introduce elastic deformation, particularly as the disc is not perfectly flat, so it will deform elastically. However, the tightening torque is kept under control to avoid any matting of the disc (and therefore plastic deformation) This design must make it possible to observe significant deformations of the part (of

the order of 0.1 mm) during each operation, in particular when there are internal stresses before machining,

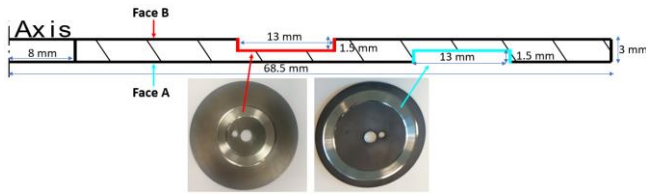


Fig. 1 Workpiece cross section - Dimension and Geometry

The whole experimental setup is shown Fig.2 and Fig. 3. The disk (in purple) is held against the plate by a clamp (outer ring). Three sensors are used during experimentation. Firstly, a piezoelectric dynamometer plate (Kistler-Type 9121A) to perform in-process cutting forces measurement. Secondly, a profilometer laser measuring system (Keyence-LJ-V7060) is used to carry out *in situ* measurement of the front plate of the disk. Its repeatability is equal to 5  $\mu$ m and resolution equal to 20  $\mu$ m in Z axis (Lathe axis). Lastly, two laser point sensors (Micro-Epsilon opto NCDT 1420) are used for *in situ* measurement of the back face and the front face simultaneously. Therefore, by combining the two sensors it is possible to evaluate the profile of the disks and its thickness. Consequently, these measurements allow the detection of possible undercut or overcut.

The cutting tests are performed on a disk on a 3-axis CNC lathe [w C' f Z X t]. The cutting insert is a PVD micro grain (Ti,Al)N + TiN coating specially designed for the finishing of superalloys (SECO RCMT0803M0-F2, CP200). Flood cooling conditions are applied using a water-based emulsion with 5% oil content by volume. The tool holder has lubrication from the centre. Thus, the coolant is directly applied on the cutting edge which provides better cooling than using a nozzle.

### 2.1. Workpiece holder-clamping system

The workpiece holder allows the positioning and clamping of the disk. with the inner (holding ring) and holding ring outer clamps. The inner clamping is insured by

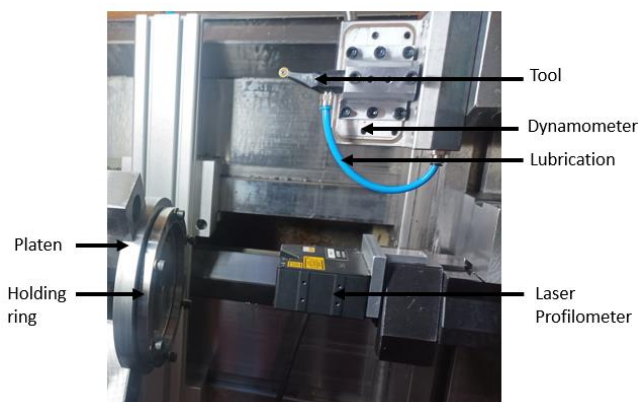


Fig. 2 Experimental set up with laser profilometer

using a washer and a screw. The platen-has 3 oblong holes

allowing for the measurement every 120° of the disk rear face.

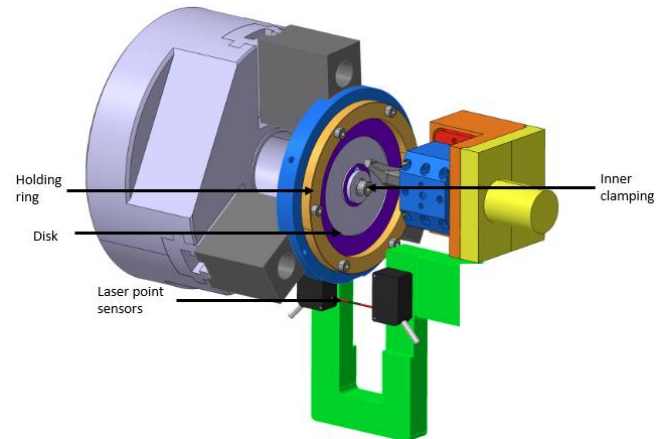


Fig. 3 Experimental setup with point-laser

### 2.2. Cutting conditions:

The cutting conditions (Table 1) are chosen according to the industrial case study and jointly with previous study of [13]. This choice is done to limit tool wear and by consequence reduce the limitation of introduction of residual stresses due to machining as shown by [19] under the same conditions as this study, that the use of a new tool reduces the introduction of residual machining stresses. With a worn tool, the thickness affected is 2.5 times less and the compression peaks are half as large. On the other hand, the change in the surface traction peak is limited.

Table 1 Cutting Conditions

$V_c$ (m/min)	$a_p$ (mm)	$f$ (mm/rev)
52.5	0.5	0.1

### 2.3. Test procedure

The disk in the machine-tool has 3 states:

- Unclamped: the disk is simply held by a centring sleeve and is placed against the platen.
- Externally: clamped disk is maintained with the holding ring only (Fig. 3)
- Full clamped: an inner clamping is added (Fig. 3)

The flowchart shown in Fig. 4 presents the sequence of a test. Changes can be implemented as shown in Fig. 5 where inner clamping is added at each step to maintain the disk against the platen.

Before the test each disk is measured by using an off-line measuring system such as Talyrond 585 round test machine. This allows one to determine the flatness of each face as well as the parallelism between them and to have a geometric reference state. The first step consists in positioning the disk on the plate with a sleeve (step 1). A first measurement step is carried out in the "unclamped" state. This check consists of a scan of the front face using the laser profilometer and a scan, between the jaws, at 3 angles at 120° of the profile of

the front and back face by using the laser point sensors through platen oblong holes.

Then, step 2 consists of applying the holding ring to retain the workpiece against the plate. Once again, a geometric check is carried out using the two laser point sensors and profilometer. These controls allow one to measure the deformation induced by the clamping.

Finally, the step 3 clamps the workpiece in the centre also. This is particularly useful if the disk has a convex shape after step 2.

The 1<sup>st</sup> machined groove is the one located on the large radius. This operation is divided in 3 passes. *In situ* measurements are made at the end of each pass in order to identify distortion after machining. Once the machining is complete, operations 4, steps 5 and 6 (Fig. 5) consist of disassembly the workpiece. Once again, measurements of each disk are performed in order to compare the disk geometry at each step. In step 7 (Fig. 5) the disk is turned over; the machined side is positioned against the plate (and thus becomes the back side). The process described previously is repeated to obtain the final geometry shown in Fig. 1. Checks are always carried out at each step. Finally, once the machining process is completed and the workpiece

is disassembled, a measurement is carried out using the Talyrond machine.

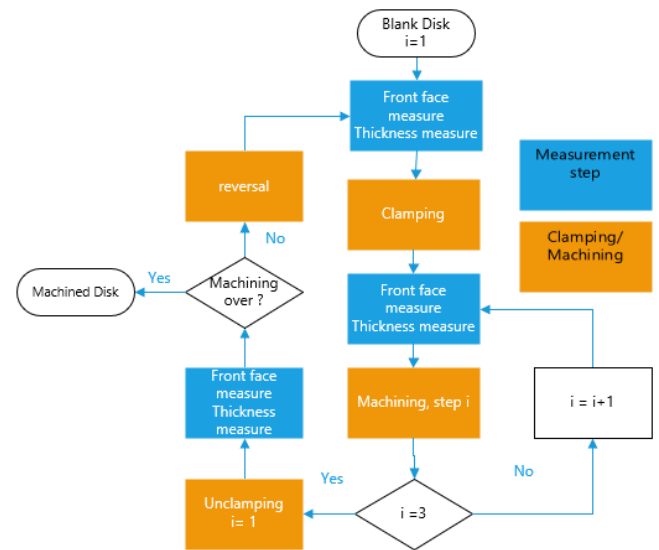


Fig. 4 Test procedure with external clamping

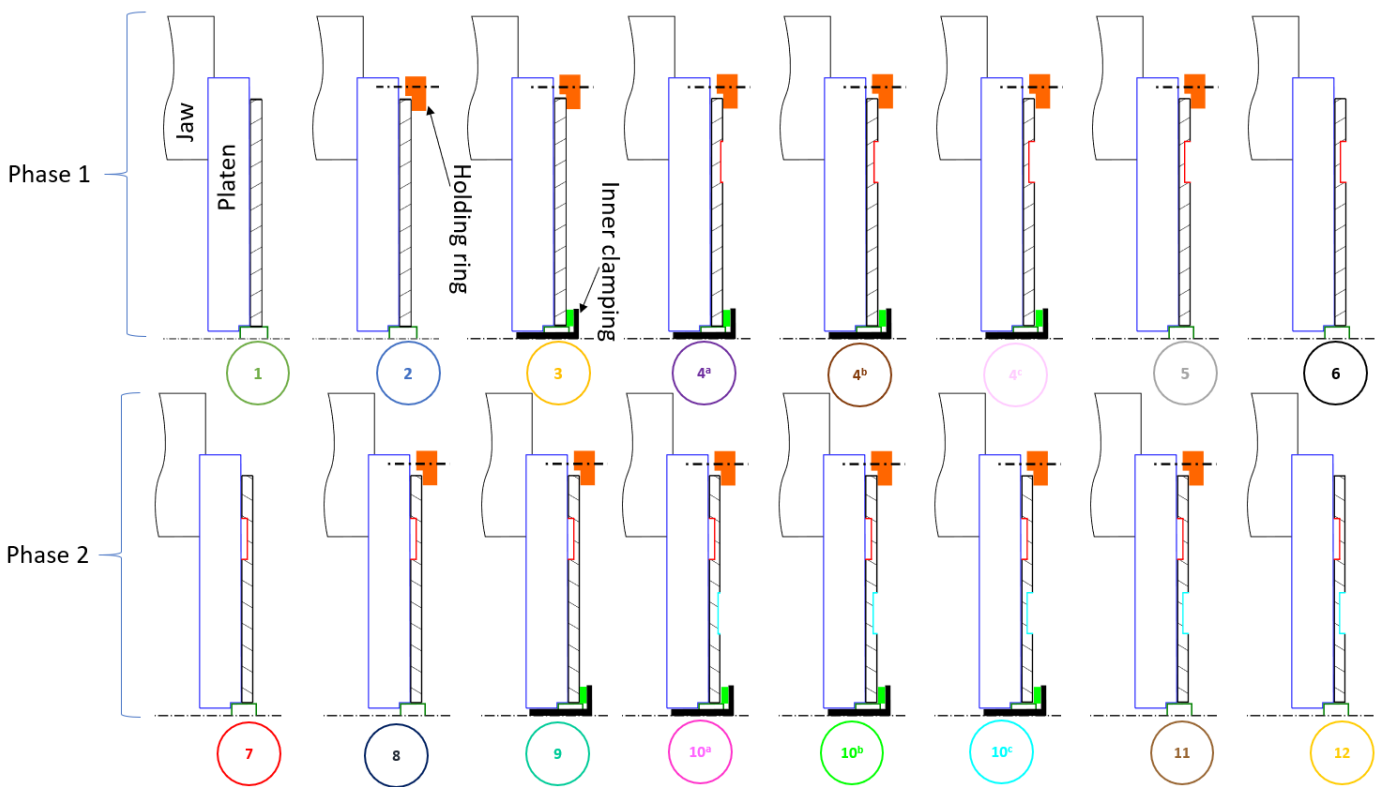


Fig. 5 . Test procedure with inner and holding ring

### 3. Experimental set-up

In this section, the results for one disk are presented after the process described in section 2 and illustrated in Fig. 5. The studied disk does not present, a priori, significant internal residual stresses. To have this internal state we have followed the procedure introduced and validated in [13]. Off-line measurements before the machining step determined that

the faces had a flatness defect of 100  $\mu\text{m}$  (Face A) and 70  $\mu\text{m}$  (Face B). This allows the deformation during the disassembly operation to be quantified.

Fig. 6 shows the geometry of the clamped disk with outer ring, but without the inner ring yet in place. The disk has a curved defect of the order of 0.2 mm maximum at its centre. The use of the inner ring means that the disk can be pressed more firmly against the platen. Fig. 7 shows the result, the disk



seems to have a better flatness. A further analysis is carried out using laser point sensors in the following paragraph.

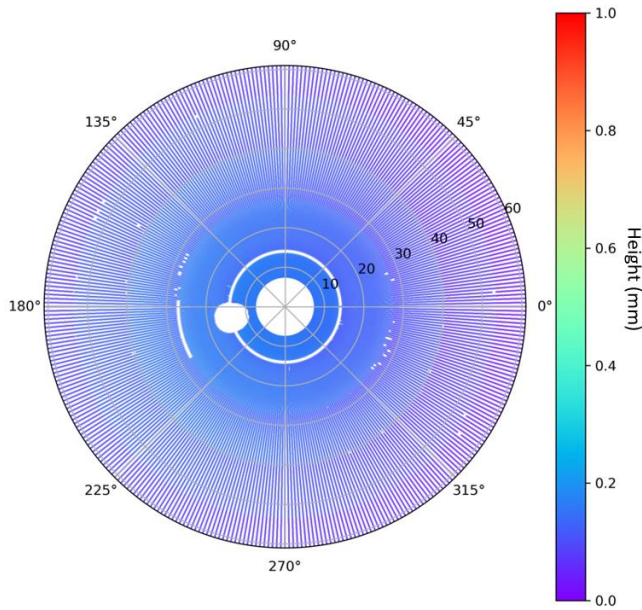


Fig. 6 Scan of the disk geometry in step 1: front face, face A

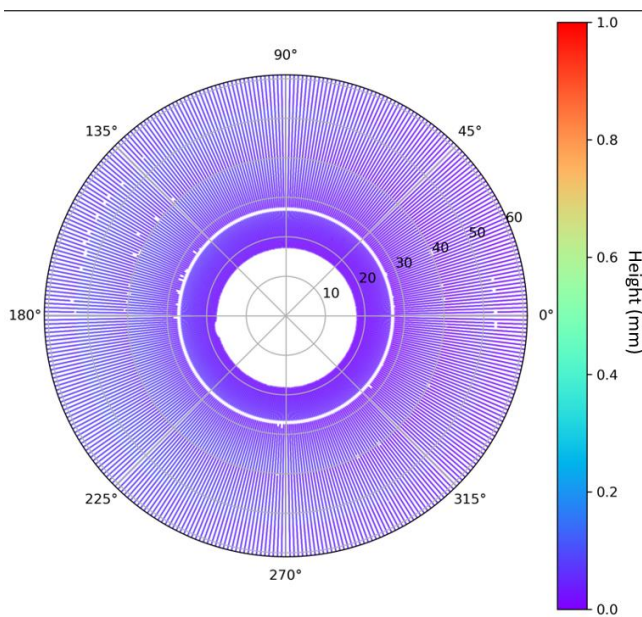


Fig. 7 Scan of the disk geometry in step 2: front face, face A

### 3.1. Result after machining step 1

The evolution of the position of the back face of the disk during machining step 1 is shown in Fig. 8. The curve number corresponds to the step described in Fig. 5. Curve 2 represents the geometrical state of the disk when it has just been clamped by the holding ring. Thus, it is slightly bulging towards the centre. When the inner clamp is put in place (curve 3), the disk is against the plate, but seems to retain a slight curvature. So, despite the impression given by Fig. 7, the disk does not appear to be perfectly flat before machining (for its back face). The disk does not move during the machining process (curve 4a, 4b, 4c) and then, when the inner clamping is removed, it returns back, but slightly deformed in relation to

the initial geometry (curve 5). Thus, the disk does not seem to have been deformed during machining.

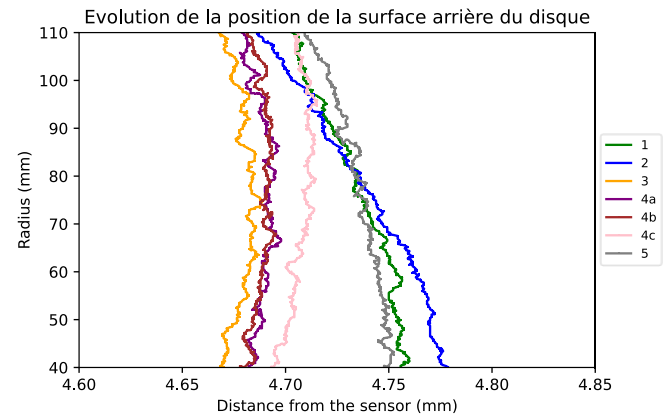


Fig. 8 Evolution of the position of the back face (face B) in Machining step 1

The previous observations are confirmed by the Fig. 9. Indeed, the curves represent the shape deviation between two successive steps for the back face of the disk (which is not machined during this step). This enables the chronology of the deformations to be determined. This is more interesting than simply comparing before and after machining. Thus, the disk is deformed by 0.12 mm during the inner clamping (curve 3-2) and the disk does not come back into place as shown by Fig. 8 and Fig. 9. The machining seems to have no consequences on the geometric state of the workpiece.

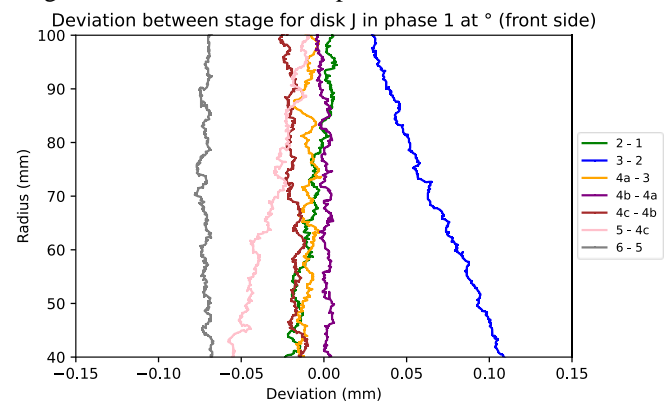


Fig. 9 Shape deviation of back face (face B) between two successive operations in machining step 1

The fact of carrying out the machining only slightly deforms the disk, since the deviation observed is of the order of a micron (curves 4a-3, 4b-4a, 4c-4b). It is therefore difficult to interpret anything about this. On the other hand, when the central clamp is removed, there is a slight deformation of the order of a few microns (curve 5-4c). The disk has therefore been permanently deformed during the process as it does not return to its initial geometry.

Fig. 10 exposes the results of the laser point on the front face of the disk for machining step 1. Here again, this figure exposes the difference in shape between two successive steps. In fact, the front face and the back face may not behave in the same way during the process. Fig. 10 confirms that the

behaviour is similar. Curve 3-2 clearly shows the same deformation when the inner ring was added, while curves 4a-3, 4b-4a, 4c-4b confirm that the machining did not introduce any additional quantifiable defects, since the deviations observed are of the order of a micron. Finally, curve 5-4c shows that the disk has not returned to its initial geometric shape.

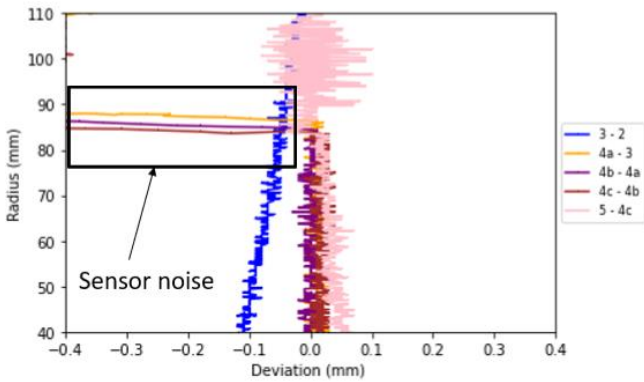


Fig. 10 Shape deviation between two successive operations in machining step 1 (front face, face A)

### 3.2. Results after machining step 2

The part is unclamped, then turned around. Face A becomes the front face and inversely. The same operations are repeated as in machining step 1, in accordance with the process described in Fig. 5. The evolution of the position of the back face of the disk during machining step 2 is depicted in Fig. 11. Curve 8 shows that the disk is curved and therefore not plated when it is clamped only with the outer ring. Curve 9 describes the geometric state of the disk after the inner ring has been fitted. The disk is almost flat, having undergone a displacement of approximately 0.25 mm when the flange was added. This displacement is much greater than the displacements observed during the unclamping step for the inner clamp in machining step 1, since it was only a few microns. The machining steps do not appear to introduce deformations as seen in machining step 1. Indeed, the curves 10a/b/c are superimposed. Finally, during the unclamping step, the part almost returns to its initial shape, since curves 8 and 11 are almost superimposable.

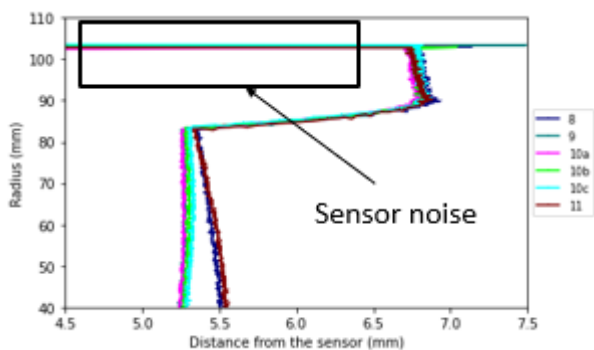


Fig. 11 Shape deviation in machining step 2 (back face, face A)

The observations in Fig.11 are confirmed by Fig. 12 which shows the difference between two successive steps for machining step 2. Thus, at the lowest point measured, a distortion of almost 0.25 mm is applied to the disk during the

inner clamping. However, this deformation seems to be purely elastic, as the same deviation is found when the inner clamping is removed. As in machining step 1, there seems to be no distortion during machining. This is again due to the presence of a very small internal residual stress gradient.

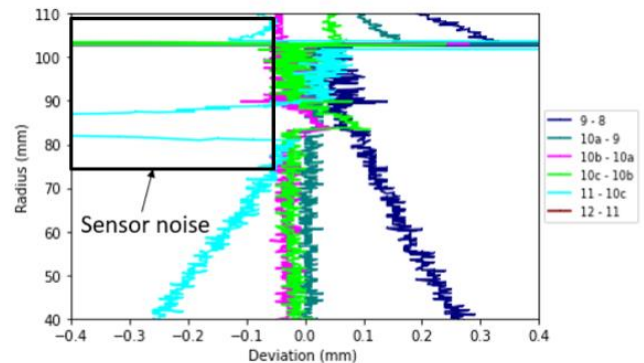


Fig. 12 Shape deviation between two successive steps in machining step 2 (back face, face A)

The disk appears to take on a concave shape from the start of the second machining step and throughout the rest of the process. This is confirmed by the results shown in Fig. 13. This figure shows the difference in shape between the externally clamped and internally clamped disks on the front face. The displacements are significant close to the centre. At the 20 mm radius, the data is identical to that of the laser point sensors, with a displacement close to 0.25 mm.

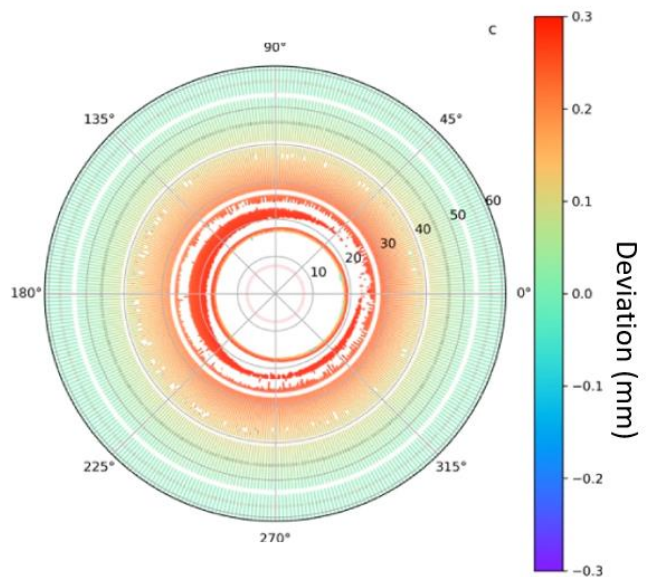


Fig. 13 Shape deviation between inner clamping and disassembly steps in machining step 2 (Face B)

## 4. Conclusion

This study focuses on a methodology for characterising the effect of clamping and stresses induced by machining for thin Inconel 718 workpiece. The results show that phenomena occur during the clamping and unclamping steps. The observed distortions at the end of machining step 2 are not identical to the post-machining analysis of the disks. This is explained in

particular by the difficulty of measuring the disks in the unclamped state on the machining fixture. In fact, a rigid body movement occurred during unclamping. This results in the disk moving and leaving the measurement sensitivity zones. Difficulties were also encountered in aligning the disks with a reference surface. New tests will therefore be carried out to take account of the difficulties encountered. For example, off-line measurements, performed with Talyrond 585, will be introduced at the end of step 6 (end of machining step 1) to enable improved monitoring of the geometric evolution of the specimen.

For next studies tests will involve specimens with an internal residual stress profile that will first be measured by XRD. Some workpiece will be measured after machining and others before. The workpieces have an initial thickness of 3 mm. XRD analysis can be carried out to a depth of almost 1 mm, which will give a good estimate of the internal residual stress field. In the case of a machined disc, it should be possible to obtain the machining residual stress field over almost the entire thickness. These tests will corroborate the analyses carried out using the MORFEO finite element software to make progress in multi- step machining modelling. They will also be used to test different clamping configurations to further enhance their effect (multiplying unclamping and clamping steps).

## 5. References

- [1] Li, W., Withers, P.J., Axinte, D., Preuss, M., Andrews, P., 2009. Residual stresses in face finish turning of high strength nickel-based superalloy. *Journal of Materials Processing Technology* 209, 4896–4902. <https://doi.org/10.1016/j.jmatprotec.2009.01.012>
- [2] Huang, X., Sun, J., Li, J., 2015. Finite element simulation and experimental investigation on the residual stress-related monolithic component deformation. *Int J Adv Manuf Technol* 77, 1035–1041. <https://doi.org/10.1007/s00170-014-6533-9>
- [3] Schulze V, Arrazola P, Zanger F, Osterried J (2013) Simulation of distortion due to machining of thin-walled. In: *Proceedings of the 14th CIRP Conference on Modeling of Machining Operations.*, pp 845–50. [doi:10.1016/j.procir.2013.06.063](https://doi.org/10.1016/j.procir.2013.06.063)
- [4] Ma K, Goetz R, Svrivatsa S (2010) *ASM Handbook. Metals Process Simulation* 22B:386–402
- [5] Liu, L., Sun, J., Chen, W., Zhang, J., 2017. Finite element analysis of machining processes of turbine disk of Inconel 718 high-temperature wrought alloy based on the theorem of minimum potential energy. *Int J Adv Manuf Technol* 88, 3357–3369. <https://doi.org/10.1007/s00170-016-9026-1>
- [6] Denkena, B., Boehnke, D., de León, L., 2008. Machining induced residual stress in structural aluminum parts. *Prod. Eng. Res. Devel.* 2, 247–253. <https://doi.org/10.1007/s11740-008-0097-1>
- [7] Iheb Cherif. Modélisation et validation expérimentale de la distorsion de plaques usinées. Autre [cond-mat.other]. Ecole nationale supérieure d'arts et métiers - ENSAM, 2019. In French.
- [8] Nixon et al., 1971] Frank Nixon, 1971. *Managing to Achieve Quality and Reliability*. Frank Nixon. McGraw-Hill, 1971. 290 pp.\pounds 4.25. *The Aeronautical Journal*. Vol. 75, n° 731, pp. 796–796
- [9] Croppi, L., Grossi, N., Scippa, A., Campatelli, G., 2019. Fixture Optimization in Turning Thin-Wall Components. *Machines* 7, 68. <https://doi.org/10.3390/machines7040068>
- [10] Gonzalo, O., Seara, J.M., Guruceta, E., Izpizua, A., Esparta, M., Zamakona, I., Uterga, N., Aranburu, A., Thoelen, J., 2017. A method to minimize the workpiece deformation using a concept of intelligent fixture. *Robotics and Computer-Integrated Manufacturing* 48, 209–218. <https://doi.org/10.1016/j.rcim.2017.04.005>
- [11] Li, Y., Liu, C., Hao, X., Gao, J.X., Maropoulos, P.G., 2015. Responsive fixture design using dynamic product inspection and monitoring technologies for the precision machining of large-scale aerospace parts. *CIRP Annals* 64, 173–176. <https://doi.org/10.1016/j.cirp.2015.04.025>
- [12] Zhang, Z., 2020. A new in-processes active control method for reducing the residual stresses induced deformation of thin-walled parts. *Journal of Manufacturing Processes* 10.
- [13] Bastien Toubhans. Caractérisation et modélisation des distorsions en tournage de pièces minces en Inconel 718. Génie mécanique [physics.class-ph]. HESAM Université, 2020. In French
- [14] Cantero, J.L., Díaz-Álvarez, J., Miguélez, M.H., Marín, N.C., 2013. Analysis of tool wear patterns in finishing turning of Inconel 718. *Wear* 297, 885–894. <https://doi.org/10.1016/j.wear.2012.11.004>
- [15] Costes, J.P., Guillet, Y., Poulachon, G., Dessoly, M., 2007. Tool-life and wear mechanisms of CBN tools in machining of Inconel 718. *International Journal of Machine Tools and Manufacture* 47, 1081–1087. <https://doi.org/10.1016/j.ijmachtools.2006.09.031>
- [16] Grzesik, W., Niesłony, P., Habrat, W., Sieniawski, J., Laskowski, P., 2018. Investigation of tool wear in the turning of Inconel 718 superalloy in terms of process performance and productivity enhancement. *Tribology International* 118, 337–346. <https://doi.org/10.1016/j.triboint.2017.10.005>
- [17] Zhu, D., Zhang, X., Ding, H., 2013. Tool wear characteristics in machining of nickel-based superalloys. *International Journal of Machine Tools and Manufacture* 64, 60–77. <https://doi.org/10.1016/j.ijmachtools.2012.08.001>
- [18] Madariaga, A., Esnaola, J.A., Fernandez, E., Arrazola, P.J., Garay, A., Morel, F., 2014. Analysis of residual stress and work-hardened profiles on Inconel 718 when face turning with large-nose radius tools. *Int J Adv Manuf Technol* 71, 1587–1598. <https://doi.org/10.1007/s00170-013-5585-6>
- [19] Toubhans, B., Fromentin, G., Viprey, F., Karaoui, H., Dorlin, T., 2020. Machinability of inconel 718 during turning: Cutting force model considering tool wear, influence on surface integrity. *Journal of Materials Processing Technology* 285, 116809. <https://doi.org/10.1016/j.jmatprotec.2020.116809>